DALTON
FULL PAPER

# Crystalline TCNQ and TCNE adducts of the diborane(4) compounds $B_2(1,2\text{-}E_2C_6H_4)_2$ (E = O or S)

**Todd B. Marder,[a] Nicholas C. Norman,*[b] A. Guy Orpen,*[b] Michael J. Quayle †[b] and Craig R. Rice[b]**

[a] *The University of Durham, Department of Chemistry, Science Laboratories, South Road, Durham, UK DH1 3LE*
[b] *The University of Bristol, School of Chemistry, Cantock's Close, Bristol, UK BS8 1TS*

***Received 11th February 1999, Accepted 12th May 1999***

Crystal structures of 1 : 1 adducts of diborane(4) compounds and the electron acceptors TCNQ and TCNE, namely $B_2(1,2\text{-}E_2C_6H_4)_2$·TCNQ (E = O or S) and $B_2(1,2\text{-}E_2C_6H_4)_2$·TCNE (E = O or S), have been found to show predominantly two-dimensional heteromolecular packing motifs with a variety of interlayer packings.

Charge transfer complexes of electron rich alkenes, such as tetrathiafulvalene [2-(1,3-dithiol-2-ylidene)-1,3-dithiole] (TTF) and tetramethyltetraselenafulvalene (TMTSF), and electron acceptors, such as TCNQ **1** (7,7,8,8-tetracyano-*p*-quinodimethane) and TCNE **2** (tetracyanoethene), constitute an important and much studied class of crystalline organic material with important properties including metallic conductivity and superconductivity.[1] Another electron rich alkene to have been studied in this regard, although one which affords materials with significantly less satisfactory electronic properties,[1] is dibenzotetrathiafulvalene **3**, together with its selenium and tellurium analogues **4** and **5**. The structure of the adduct **3·1** has been established by X-ray crystallography.[2] In view of the close structural relationship between compound **3** and the diborane(4) compound $B_2(1,2\text{-}S_2C_6H_4)_2$ **6** (they differ by only two electrons), and with the related oxo-derivative $B_2(1,2\text{-}O_2C_6H_4)_2$ **7**,[3] we sought to investigate whether **6** and **7** would form similar crystalline adducts with TCNQ and TCNE and to explore the nature of the intermolecular interactions.

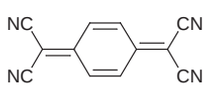


**1**

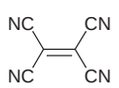


**2**

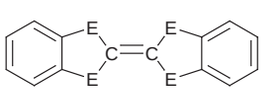


**3**, E = S; **4**, E = Se; **5**, E = Te

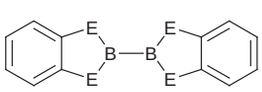


**6**, E = S; **7**, E = O

## Results and discussion

A solution of equimolar quantities of compounds **6** and **1** in $CH_2Cl_2$ showed no colour change (**6** is colourless, **1** is pale yellow) and $^1H$ and $^{11}B$ NMR analysis provided no evidence for any adduct formation in solution.[4,‡] However, cooling to −30 °C afforded dark red crystals of the 1 : 1 adduct **6·1a**. Red crystals of the 1 : 1 adducts **6·2**, **7·1** and **7·2** were prepared similarly. In addition, by employing 1,2-dichloroethane as a solvent, a second polymorphic form of **6·1a** (**6·1b**) was also crystallised. Full experimental details and analytical data are provided in the Experimental section.

† *Present address*: Department of Chemical Engineering, UMIST, PO Box 88, Manchester, UK M60 1QD.
‡ The proton and boron solution chemical shifts of compounds **6** and **7** shift markedly upfield when the boron centres are complexed by nitrogen (and phosphorus) donor ligands as discussed in ref. 4.

All five crystal structures are notably similar, having the triclinic space group $P\bar{1}$ with $Z = 1$. The component molecules each lie over an inversion centre and the unit cell volumes are 576.3, 582.0, 516.8, 470.5 and 419.2 Å$^3$ for **6·1a**, **6·1b**, **7·1**, **6·2** and **7·2**, respectively. The crystal structure of **3·1** which has been previously characterised[2] also crystallises in the space group $P\bar{1}$ with $Z = 1$ and a unit cell volume of 574.9 Å$^3$. Selected crystallographic details for all structures are given in Table 1.

All six crystal structures (*i.e.* the five described here and **3·1**) show a predominant two-dimensional packing in which the layers consist of the component species in a 1 : 1 ratio. In the third dimension, the crystal structures contain an ABCABC packing arrangement in which the layers are stacked parallel above each other along the crystallographic *c* axis direction. Despite the overall similarity of the structures, however, the two-dimensional arrangements of the component molecules do differ between each structure, utilising a range of intermolecular interactions to pack efficiently. The two-dimensional crystal structures for **6·1a**, **3·1**, **7·1**, **6·2** and **7·2** are shown in Figs. 1–5 respectively. A discussion for each is given first followed by a description of the three-dimensional packing. Simplified representations of the two-dimensional structures are shown in Fig. 6.

Common to all six crystal structures are parallel homomolecular ribbons in the crystallographic *a* direction linked by heteromolecular interactions. Intermolecular interactions were recorded with cut-off limits S···S 3.80, S···H 3.25 and N···H 2.95 Å. As shown in Fig. 7 three angles have been employed to describe the orientations of the molecules within the layers. The angle $\theta$ describes misalignment of the molecular axes relative to each other, *i.e.* the direction of propagation in the heteromolecular ribbon. This has been calculated as the angle between the molecular axes of each species [through the B–B bond for **6** and **7**, through the C=C($CN_2$) unit for **1** and through the C=C bond for **2**]. The angles $\omega$ and $\varphi$ ($\varphi'$ is used for **2**) describe the angle of propagation of the homomolecular ribbons. These are calculated as the angle between the molecular axis of one molecule and the line relating an atom in one molecule to the corresponding atom in the next molecule in the homomolecular ribbon, *i.e.* the *a* axis. Table 2 records these angles for each crystal structure.

The two-dimensional structures of adducts **6·1a** (Fig. 1) and **6·1b** (not shown) are essentially the same. The homomolecular ribbons of **6** are apparently driven primarily by S···S and S···H contacts, there being two S···S interactions and eight S···H contacts per molecule including a three-centred interaction between S(2), S(1a) and H(6a). The symmetry independ-

**Table 1** Selected crystallographic details for the complexes **6·1a**, **6·1b**, **7·1**, **6·2**, **7·2** and **3·1**

| | **6·1a** | **6·1b** | **7·1** | **6·2** | **7·2** | **3·1**[a] |
|---|---|---|---|---|---|---|
| Empirical formula | $C_{24}H_{12}B_2N_4S_4$ | $C_{24}H_{12}B_2N_4S_4$ | $C_{24}H_{12}B_2N_4O_4$ | $C_{18}H_8B_2N_4S_4$ | $C_{18}H_8B_2N_4O_4$ | $C_{26}H_{12}N_4S_4$ |
| Formula weight | 506.24 | 506.24 | 442.00 | 430.14 | 365.90 | 508.65 |
| Crystal system | Triclinic | Triclinic | Triclinic | Triclinic | Triclinic | Triclinic |
| Space group | $P\bar{1}$ | $P\bar{1}$ | $P\bar{1}$ | $P\bar{1}$ | $P\bar{1}$ | $P\bar{1}$ |
| $a$/Å | 7.803(3) | 7.862(2) | 7.1996(11) | 6.861(3) | 5.962(3) | 9.215(3) |
| $b$/Å | 7.855(4) | 8.386(2) | 8.560(3) | 7.172(3) | 6.024(4) | 10.644(4) |
| $c$/Å | 9.867(4) | 9.745(2) | 9.414(3) | 10.862(3) | 12.686(6) | 7.734(2) |
| $\alpha$/° | 73.85(5) | 71.97(3) | 67.00(2) | 80.80(2) | 97.88(2) | 113.32(3) |
| $\beta$/° | 85.71(3) | 72.71(2) | 83.16(2) | 79.61(3) | 97.66(3) | 122.28(2) |
| $\gamma$/° | 83.18(3) | 88.28(2) | 75.47(2) | 64.00(2) | 108.91(3) | 67.64(3) |
| $V$/Å$^3$ | 576.3(4) | 582.0(2) | 516.8(3) | 470.5(3) | 419.2(4) | 574.9(3) |
| $T$/K | 173(2) | 173(2) | 173(2) | 173(2) | 173(2) | Room temperature |
| $Z$ | 1 | 1 | 1 | 1 | 1 | 1 |
| $\mu$/mm$^{-1}$ | 0.434 | 0.430 | 0.098 | 0.517 | 0.103 | |
| Total reflections | 4904 | 6120 | 4293 | 4889 | 2677 | |
| Independent reflections | 1963 | 2637 | 1749 | 2123 | 1847 | |
| $R_{int}$ | 0.0488 | 0.0337 | 0.0427 | 0.0398 | 0.0416 | |
| $R_1$ [$I > 2\sigma(I)$] (data) | 0.0470 (1324) | 0.0365 (1867) | 0.0547 (1164) | 0.0470 (1523) | 0.0576 (1508) | |

[a] Details taken from ref. 2.

**Table 2** Crystal packing parameters

| Adduct | $\theta$/° | $\omega$/° | $\varphi$/° | Interlayer separation/Å |
|---|---|---|---|---|
| **6·1a** | 7.3 | 54.9 | 59.5 | 3.59 |
| **6·1b** | 4.3 | 54.1 | 58.4 | 3.43 |
| **3·1** | 9.2 | 55.5 | 57.8 | 3.44 |
| **7·1** | 52.3 | 56.6 | −71.1 | 3.44 |
| **6·2** | 8.9 | 77.2 | −65.6[a] | 3.60 |
| **7·2** | 56.9 | 54.4 | 68.6[a] | 3.39 |

[a] Values given are for $\varphi'$ (see Fig. 7).

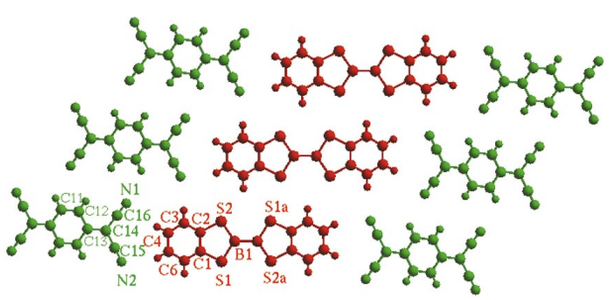


**Fig. 1** A view of the two-dimensional packing arrangement of molecules of **6** (red) and **1** (green) in adduct **6·1a** showing the atom numbering scheme. Atoms are drawn as spheres of arbitrary radius.

ent intermolecular interactions for all crystal structures are listed in Table 3 and are categorised according to the ribbon type they form. The angle of propagation $\omega$ in the homomolecular direction of **6** in **6·1a** is 54.9° [54.1° in **6·1b**] and for **1** in **6·1a** $\varphi$ is 59.5° [58.4° in **6·1b**]. These ribbons of **1** have eight C≡N · · · H contacts per molecule. The two-dimensional layers in **3·1** (Fig. 2) are similar to those in **6·1a** and **6·1b**, with homomolecular ribbons propagating at angles of $\omega = 55.5°$ and $\varphi = 57.8°$. These ribbons also contain the same intermolecular distances, with a similar length for the chalcogen-containing molecular ribbons and slightly longer (by *ca.* 0.2 Å) lengths for the ribbons of **1**. The structures of **6·1a**, **6·1b** and **3·1** show near linear heteromolecular ribbons [the molecular axes of **6** and **1** are canted at angles $\theta$ of only 7.3, 4.3 and 9.2° in **6·1a**, **6·1b** and **3·1** respectively] which contain six C≡N · · · H (<2.95 Å) contacts per molecule of **1**. Thus, it appears that the homomolecular interactions are at least numerically dominant in these crystal structures as indicated by the greater number of interactions formed in the homomolecular directions. The layers are slightly ruffled with the angle between the mean

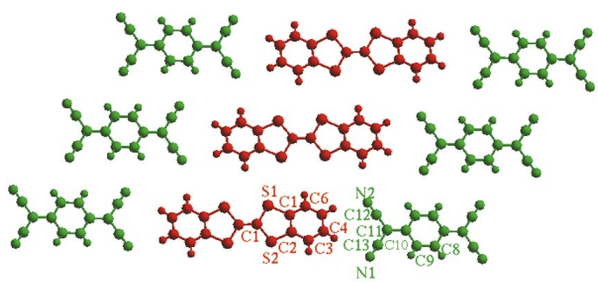


**Fig. 2** A view of the two-dimensional packing arrangement of molecules of **3** (red) and **1** (green) in adduct **3·1**. Details as in Fig. 1.

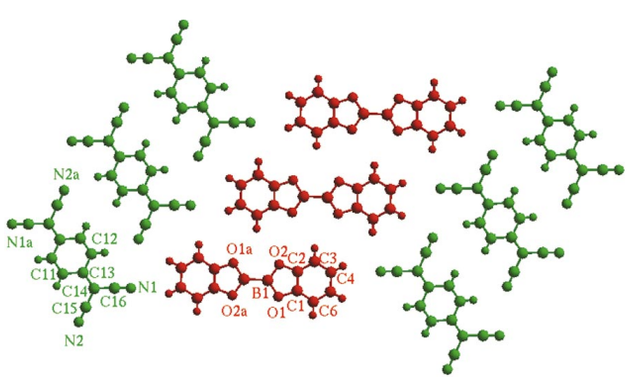


**Fig. 3** A view of the two-dimensional packing arrangement of molecules of **7** (red) and **1** (green) in adduct **7·1**. Details as in Fig. 1.

planes through **6** and **1** being 11.9, 10.9 and 3.6° in **6·1a**, **6·1b** and **3·1** respectively.

In adduct **7·1** (Fig. 3) the arrangement of molecules of **7** is similar to those of **6** in **6·1**, with an angle of propagation $\omega$ of 56.6° [*cf.* 54.9° in **6·1a**]. Thus there are two O · · · O and eight O · · · H–C contacts per molecule and the three-centred H · · · E interaction is also present. Molecules of **1** propagate at similar magnitudes of $\varphi$ (−71.1°, *cf.* 59.5° in **6·1a**), but rotated in the opposite sense. As a result there are only four short C≡N · · · H contacts per molecule rather than eight. The lateral displacement of molecules of **1** in the direction orthogonal to the homomolecular axis precludes the interaction N(2) · · · H(11A) (present in **6·1a**). The main difference in the two crystal structures lies in the angle of propagation along the heteromolecular chains, which are less linear in **7·1** ($\theta = 52.3°$) [*cf.* 7.3° in **6·1a**]. Thus, the heteromolecular ribbons are better termed zigzag, although as in **6·1a** and **6·1b** they extend along the crystallographic $b$ axis and contain six C≡N · · · H–C contacts per

**Table 3** Selected intermolecular distances for adducts **6·1a**, **6·1b**, **3·1**, **7·1**, **6·2** and **7·2**

| | **6·1a** | | **6·1b** | | **3·1** | |
|---|---|---|---|---|---|---|
| **A**[a] | S1 · · · S1$^{i}$ | 3.582(2) | S1 · · · S1$^{i}$ | 3.613(1) | S2 · · · S2$^{i}$ | 3.716 |
| **A** | S2 · · · H6$^{ii}$ | 3.177(4) | S2 · · · H6$^{ii}$ | 3.236(2) | S1 · · · H3$^{ii}$ | 2.904 |
| **A** | S1 · · · H6$^{ii}$ | 3.245(4) | S1 · · · H6$^{ii}$ | 3.193(2) | S2 · · · H3$^{i}$ | 3.277 |
| **B** | N1 · · · H11$^{iii}$ | 2.653(4) | N1 · · · H11$^{iii}$ | 2.682(3) | N1 · · · H8$^{iii}$ | 2.913 |
| **B** | N1 · · · H12$^{iii}$ | 2.860(5) | N1 · · · H12$^{iii}$ | 2.731(3) | N1 · · · H9$^{iii}$ | 2.874 |
| **C** | N1 · · · H4 | 2.906(5) | N1 · · · H4 | 2.926(3) | N1 · · · H5$^{iv}$ | 2.997 |
| **C** | N2 · · · H5 | 2.708(5) | N2 · · · H5 | 2.751(3) | N2 · · · H4$^{iv}$ | 2.592 |
| **C** | N2 · · · H3$^{iv}$ | 2.679(5) | N2 · · · H3$^{iv}$ | 2.625(3) | N2 · · · H6$^{v}$ | 2.770 |
| | **7·1** | | **6·2** | | **7·2** | |
| **A** | O1 · · · H3$^{i}$ | 2.995(3) | S1 · · · S1$^{i\,b}$ | 3.578(2) | O1 · · · H3$^{i}$ | 2.685(3) |
| **A** | O2 · · · H3$^{ii}$ | 3.047(4) | S1 · · · S2$^{ii}$ | 4.064(2) | O2 · · · H3$^{ii}$ | 2.702(3) |
| **A** | O2 · · · O2$^{ii}$ | 3.805(3) | S2 · · · H6$^{iii}$ | 3.366(3) | O1 · · · O1$^{i}$ | 3.491(4) |
| **B** | N2 · · · H12$^{iii}$ | 2.572(3) | CN · · · CN$^{c}$ | 3.231 | CN · · · CN$^{c}$ | 3.239 |
| **C** | N1 · · · H4$^{iv}$ | 2.737(4) | N8 · · · H4$^{iv}$ | 2.624(4) | N8 · · · H5$^{iii}$ | 2.603(3) |
| **C** | N2 · · · H5$^{v}$ | 2.684(4) | N8 · · · H5$^{v}$ | 2.831(4) | N9 · · · H4 | 2.787(3) |
| **C** | N1 · · · H6$^{v}$ | 2.833(4) | N9 · · · H3$^{vi}$ | 2.922(4) | N9 · · · H6$^{iv}$ | 2.763(3) |
| **C** | | | N9 · · · H5$^{vi}$ | 2.658(4) | | |

[a] Letter types refer to homomolecular interactions (**A**) [for **3**, **6** and **7**] and (**B**) [for **1** and **2**] or heteromolecular interactions (**C**). Symmetry codes: **6·1a**, *i* 1 − *x*, 2 − *y*, −*z*, *ii* −1 − *x*, *y*, *z*, *iii* 1 − *x*, −1 − *y*, 1 − *z*, *iv* 1 + *x*, *y*, *z*; **6·1b**, *i* −*x*, −*y*, 2 − *z*, *ii* 1 + *x*, *y*, *z*, *iii* 1 − *x*, −1 − *y*, 1 − *z*, *iv* −1 + *x*, *y*, *z*; **3·1**, *i* *x*, *y*, −1 + *z*, *ii* −*x*, −*y*, −1 + *z*, *iii* 1 − *x*, −*y*, −1 − *z*, *iv* 1 − *x*, 1 − *y*, −*z*, *v* 1 − *x*, 1 − *y*, 1 − *z*; **7·1**, *i* −1 − *x*, *y*, *z*, *ii* −*x*, 2 − *y*, 1 − *z*, *iii* 1 + *x*, *y*, *z*, *iv* −*x*, −*y*, 1 − *z*, *v* 1 − *x*, −*y*, 1 − *z*; **6·2**, *i* 2 − *x*, −*y*, −*z*, *ii* −1 + *x*, *y*, *z*, *iii* −1 + *x*, 1 + *y*, *z*, *iv* 1 − *x*, −1 − *y*, 1 − *z*, *v* 2 − *x*, −1 − *y*, 1 − *z*, *vi* *x*, 1 + *y*, *z*, *vii* *x*, −1 + *y*, *z*; **7·2**, *i* −*x*, 1 − *y*, 1 − *z*, *ii* 1 + *x*, 1 + *y*, *z*, *iii* 2 − *x*, −*y*, 2 − *z*, *iv* −1 − *x*, −1 + *y*, *z*. [b] Interlayer contact. [c] Calculated as the distance between the midpoint of each C≡N group.

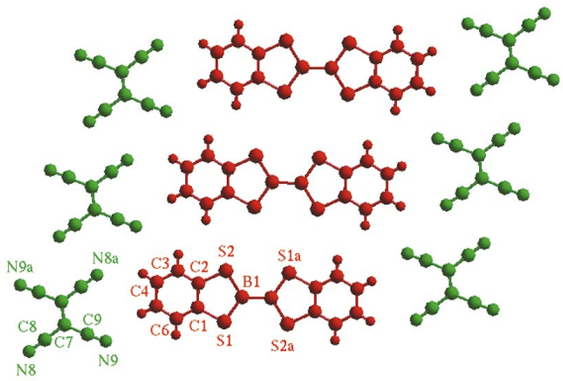


**Fig. 4** A view of the two-dimensional packing arrangement of molecules of **6** (red) and **2** (green) in adduct **6·2**. Details as in Fig. 1.

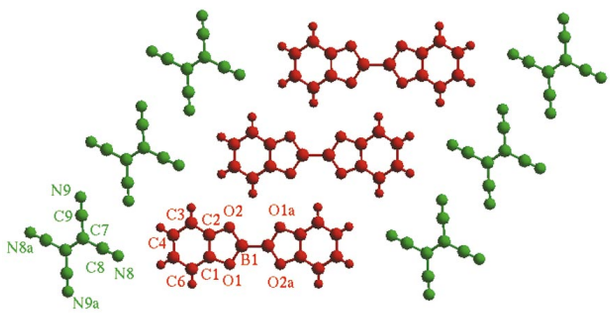


**Fig. 5** A view of the two-dimensional packing arrangement of molecules of **7** (red) and **2** (green) in adduct **7·2**. Details as in Fig. 1.

molecule. The layers remain planar, however, as in **6·1a** with the angle between the two mean planes of **7** and **1** being only 6.8°.

Homomolecular ribbons are also present in adduct **6·2** (Fig. 4) and the two-dimensional layer is similar to that observed in **6·1a**, although the angle of propagation for molecules of **6**, $\omega$, is somewhat more inclined (77.2°, *cf.* 54.9° in **6·1a**). This more canted structure for the ribbon results from the translation of molecules of **6** in the crystallographic *b* direction and gives rise to six S · · · S and four S · · · H–C interactions per molecule, as opposed to two S · · · S and eight S · · · H–C contacts per molecule in **6·1a**. The three-centred interaction observed in the crystal structures containing **1** is absent. Whilst the relative strengths of these interactions are not known with certainty (all are near the sum of the van der Waals radii in length), it is noted, however, that the same number is present in each case. In **6·2** molecules of **2** propagate at an angle of $\varphi = -65.6°$ resulting in antiparallel C≡N · · · C≡N interactions, which are notably absent in the crystal structures of **6·1** and **7·1**. In **6·2** $\theta$ is 8.9° leading to a near linear heteromolecular ribbon, containing eight C≡N · · · H–C contacts per molecule of **2**, more than are present in **6·1** and **7·1**.

In adduct **7·2** (Fig. 5) the homomolecular ribbons of **7** contain the same interactions as in **7·1**, and the propagation angle $\omega$ is 54.4° (*cf.* 56.6° in **7·1**), although the shortest of the

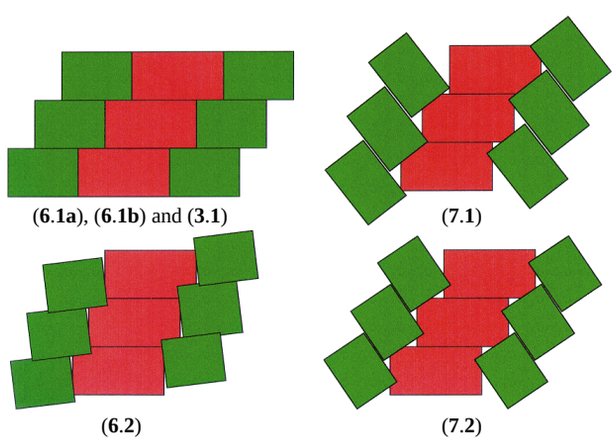


**Fig. 6** Simplified representations of the two-dimensional structures **6·1a**, **6·1b**, **3·1**, **7·1**, **6·2** and **7·2**. Molecules of **3**, **6** and **7** in red, molecules of **1** and **2** in green.

interatomic distances are shorter (by *ca.* 0.3 Å, see Table 3). Molecules of **2** in **7·2** are arranged in a different orientation from that in **6·2**, rotated by *ca.* 135° ($\varphi = -68.6$ and 65.6° for **7·2** and **6·2** respectively). The ribbons of **2** show C≡N · · · C≡N interactions as is the case in **6·2**. However, as in **7·1**, the heteromolecular ribbons are not linear, the misalignment angle $\theta$ being 56.9°, *cf.* 52.3° in **7·1**. The heteromolecular contacts

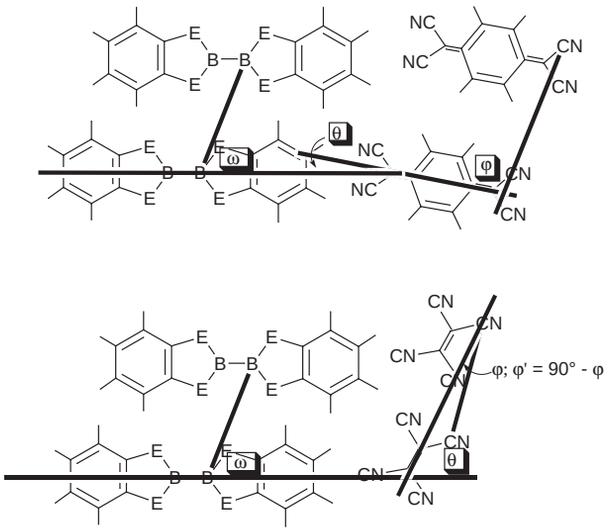


**Fig. 7** Parameters $\omega$, $\theta$, $\varphi$, $\varphi'$ used to define molecular packing in the structures of adducts **6·1a**, **6·1b**, **3·1**, **7·1**, **6·2** and **7·2**.

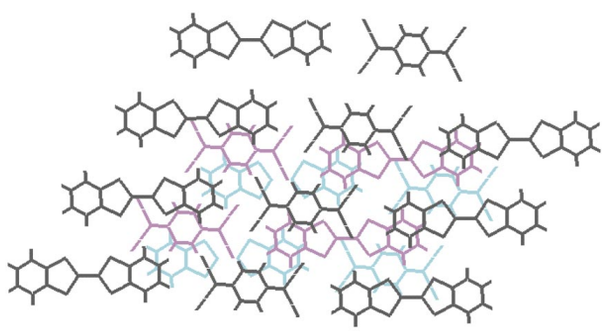

**Fig. 8** A view of three of the two-dimensional layers in adduct **6·1a** showing the three-dimensional structure (black above magenta above cyan).

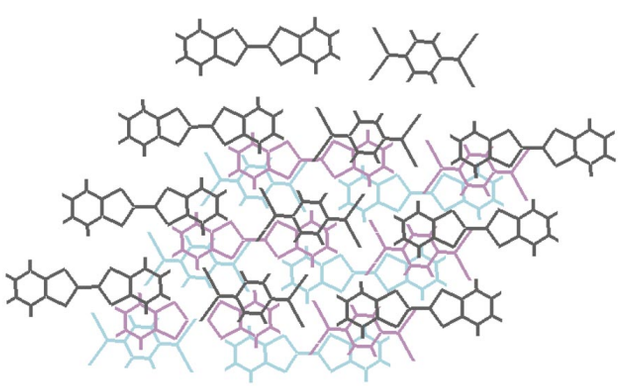

**Fig. 9** A view of three of the two-dimensional layers in adduct **6·1b**. Details as in Fig. 8.

include three short and one long C≡N · · · H–C interaction per molecule of **2**.

The layer packings in the structures of adducts **6·1a**, **6·1b**, **3·1**, **7·1**, **6·2** and **7·2** show considerable variation (see Figs. 8–13), but all have an ABCABC type packing arrangement. As noted above, the two-dimensional structures in **6·1a**, **3·1** and **6·1b** are essentially identical. It is in the third dimension that these crystal structures differ, accompanied by changes in the unit-cell volume [$V = 576.3(4)$ and $582.0(2)$ Å$^3$ for **6·1a** and **6·1b**, respectively]. In **6·1a** (Fig. 8) a degree of arene ring stacking is evident with the extremes of the arene groups of **6** being eclipsed in adjacent layers. Arene ring overlap for molecules of **1** seems unimportant, with antiparallel C≡N orientations prominent. In polymorph **6·1b** (Fig. 9) molecules of **1** again have little arene ring overlap between layers. The most notable

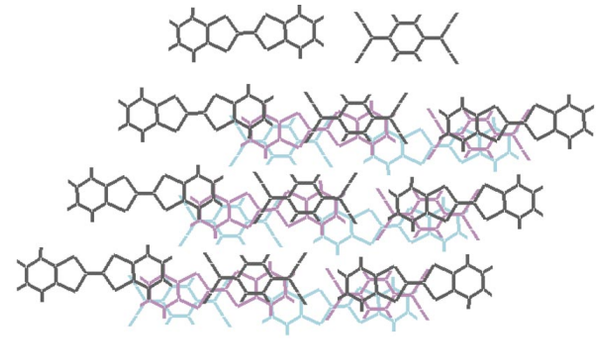

**Fig. 10** A view of three of the two-dimensional layers in adduct **3·1**. Details as in Fig. 8.

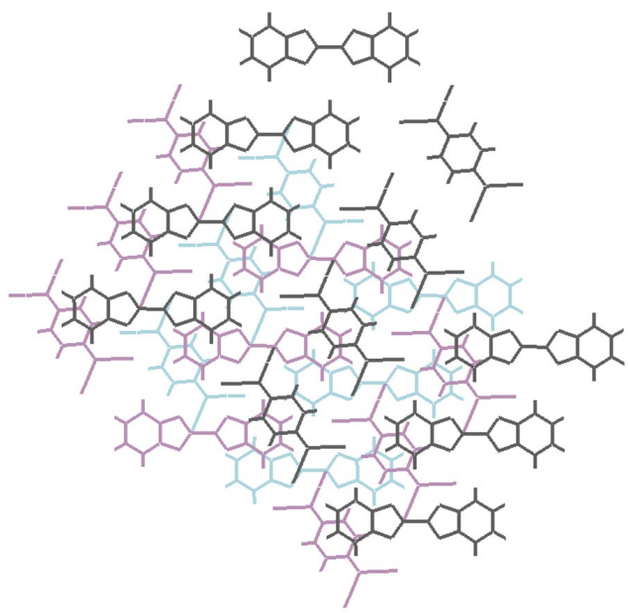

**Fig. 11** A view of three of the two-dimensional layers in adduct **7·1**. Details as in Fig. 8.

difference between the two polymorphs is that in **6·1b** there is only slight overlap of the five-membered rings of **6** and none involving their six-membered rings. Since the layers in the polymorphs are similar, **6·1b** can be described as being derived from **6·1a** by the slipping of sheets. There is a striking difference, however, in the comparison of the three-dimensional structures of both polymorphs of **6·1** with that of **3·1**. It is apparent that the heteromolecular ribbons in **3·1** (Fig. 10) align almost directly over each other, these stacks containing a multitude of heteromolecular π–π interactions with molecules of **1** sandwiched between the aromatic groups of molecules of **3** in adjacent layers.

In the structures of adducts **7·1**, **6·2** and **7·2** some degree of π stacking is apparent, but not as much as in **3·1**. In **7·1** (Fig. 11) there are some heteromolecular π stacks formed through the partial eclipsing of **7** with **1** in adjacent layers. There is no significant overlap of molecules of **6**. Heteromolecular stacking is more evident in **6·2** (Fig. 12) where molecules of **2** are sandwiched between molecules of **7**. Finally, homomolecular interlayer packing is prominent in **7·2** (Fig. 13) with the aromatic rings of molecules of **7** overlapping.

Having established that compounds **6** and **7** formed cocrystals with **1** and **2**, as is the case for **3**, it was of interest to determine the extent of any charge transfer. In **3·1** and other related crystal structures the degree of charge transfer, $z$, from the donor to the acceptor molecules, has been assessed by spectroscopic methods (IR, Raman and UV-vis) and by variations in molecular geometries.[5] In this latter method the charge transferred from the HOMO of the donor molecule (*i.e.* **3** or

**Table 4** Selected bond lengths (Å) for crystals containing compound **1**

| | **1**[a] | **6·1a** | **6·1b** | **3·1** | **7·1** |
|---|---|---|---|---|---|
| C=C (ring) | 1.346(5) | 1.339(5) | 1.343(2) | 1.346(6) | 1.337(3) |
| C–C (ring) | 1.448(4) | 1.448(5)[b] | 1.442(3)[b] | 1.442(6) | 1.450(3)[b] |
| C=C | 1.374(5) | 1.383(5) | 1.375(3) | 1.384(4) | 1.364(3) |
| C–C | 1.441(5) | 1.437(5)[b] | 1.436(3)[b] | 1.438(4)[b] | 1.441(3)[b] |
| C≡N | 1.140(5) | 1.158(4)[b] | 1.143(2)[b] | 1.138(5)[b] | 1.150(3)[b] |

[a] See ref. 6. [b] Average of two values.

**Table 5** Bond lengths (Å) for crystals containing compound **2**

| | **2**[a] | **2**[b] | **6·2** | **7·2** |
|---|---|---|---|---|
| C=C | 1.344(3) | 1.348(2) | 1.356(6) | 1.356(5) |
| C–C | 1.437(2) | 1.434(2)[c] | 1.438(4)[c] | 1.439(3)[c] |
| C≡N | 1.135(2) | 1.146(2)[c] | 1.143(4)[c] | 1.139(3)[c] |

[a] See ref. 7; cubic form. [b] Ref. 8; monoclinic form. [c] Average of two values.

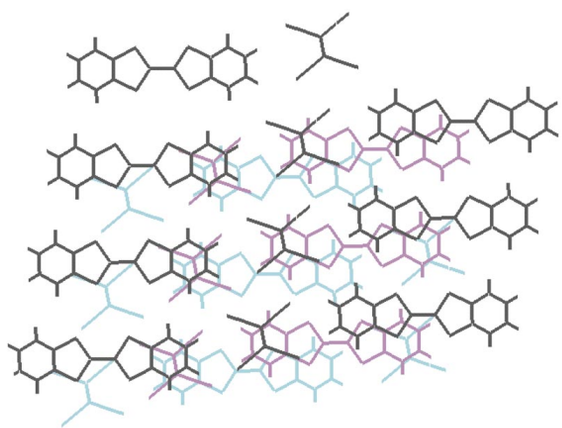

**Fig. 12** A view of three of the two-dimensional layers in adduct **6·2**. Details as in Fig. 8.

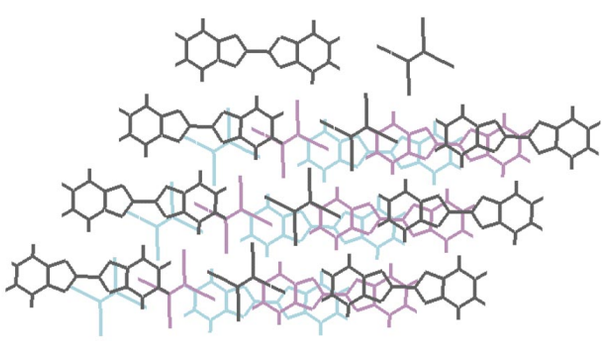

**Fig. 13** A view of three of the two-dimensional layers in adduct **7·2**. Details as in Fig. 8.

analogue) to the LUMO of the acceptor molecule (*i.e.* **1** or analogue) can be estimated by contrasting the relevant bond lengths in the crystal structures of the pure acceptor (and donor) with those in the co-crystallised materials. Such contrasts, which are supported by experiment, recognise that on population of the LUMO of TCNQ (**1**) the structure becomes more benzenoid and less quinoid in character. Similar principles hold for structures of TCNE (**2**) and its adducts. The degree of charge transfer can be evaluated in terms of the ratios of bond distances. However, as shown in Tables 4 and 5, changes in the molecular structures of **1** and **2** from the native molecule to that in the crystalline adducts reported here are negligible; selected bond lengths for the molecular stuctures of **6** and **7** in the parent structures and in the adducts are noted in

**Table 6** Bond lengths (Å) for crystals containing compound **6**

| | **6**[a] | **6·1a** | **6·1b** | **6·2** |
|---|---|---|---|---|
| B–B | 1.675(5) | 1.681(8) | 1.676(4) | 1.682(6) |
| B–S | 1.792(2) | 1.791(4)[b] | 1.791(3)[b] | 1.789(3)[b] |
| S–C | 1.756(2) | 1.754(4)[b] | 1.758(2)[b] | 1.755(3)[b] |

[a] See ref. 3(*b*). [b] Average of two values.

**Table 7** Bond lengths (Å) for crystals containing compound **7**

| | **7**[a] | **7·1** | **7·2** |
|---|---|---|---|
| B–B | 1.678(5) | 1.677(6) | 1.684(5) |
| B–O | 1.388(2) | 1.388(3)[b] | 1.389(3)[b] |
| O–C | 1.387(2) | 1.396(3)[b] | 1.384(3)[b] |

[a] See ref. 3(*b*). [b] Average of two values.

**Table 8** Lattice energies (kcal mol$^{-1}$) for experimental structures

| Adduct | Lattice energy |
|---|---|
| **6·1a** | −73.92 |
| **6·1b** | −66.80 |
| **3·1** | −63.96 |
| **7·1** | −70.43 |
| **6·2** | −63.31 |
| **7·2** | −50.95 |

Tables 6 and 7 and also show negligible changes. Thus, despite the red colour associated with the co-crystals of **6/7** with **1/2** described here, there is no structural evidence for any appreciable charge transfer although this is not unexpected due to the relatively poor electron donating ability of benzenoid derivatives such as **3** as noted in the Introduction; preliminary electrochemical studies on **6** and **7**[9] together with PES, EHMO and UV-vis results[3a] also confirm that they are poor electron donors.§ Nevertheless, the fact that the crystalline adducts described here do form indicates that boron analogues of TTF and TMTSF are worthy synthetic targets that are likely to afford crystalline adducts with **1/2** where the degree of charge transfer (and hence conductivity) may be much greater.

As a final aspect of this study, lattice energy calculations[10a,11] have been performed to evaluate and compare the relative stability of each crystal structure, particularly for the polymorphic pair **6·1a** and **6·1b**, and to assess the importance of the intermolecular interactions. The procedure followed the methods used by Buttar *et al.*[12] The results are presented in Table 8 and suggest that the packing in polymorph **6·1a** is 7.12 kcal mol$^{-1}$ more stable than that in **6·1b** (as might be expected given its higher density and lower unit cell volume). Lattice energy calculations using the experimental structure have been asserted to reproduce experimental values successfully.[10] The experimental lattice energy results for the polymorphs **6·1a** and **6·1b** appear to be consistent with current theories on differences in lattice energies between polymorphs being less than *ca.* 10% of the total lattice energy.[10b,12] Since the two-dimensional layers of **6·1a**, **6·1b** and **3·1** are essentially indentical, one might expect that the relative differences in lattice energies be associated with layer stacking and particularly to arise from favourable π–π interactions. If this were the case, **3·1** would be the most stable structure type since, as noted above, the ribbons align above each other in a more organised fashion than in **6·1a** and **6·1b**. However, the lattice energy of **3·1** is less than that of either **6·1a** or **6·1b** suggesting that arene stacking is of little

§ Measurement of the electrical conductivity of the crystalline adducts reported here has been hampered by the small size of the crystals.

importance here (at least insofar as the force fields are able to reproduce such interactions).

The apparent thermodynamic preference for the formation of co-crystals in all these cases is striking and presumably favoured by formation of heteromolecular contacts. There may, however, be (kinetic) crystallisation effects at work, since the co-crystals are presumably less soluble than the individual component species.

In view of the dominance of the two-dimensional layers and the results of the lattice energy calculations, it becomes apparent that interlayer π stacking is not important in the formation of these co-crystals. Indeed, as evidenced by the existence of polymorphs **6·1a** and **6·1b** the layers can slip at very little energy penalty. Attempted structure optimisations led to significant layer slippings, without affecting the sequence of lattice energies, and with very small effects on the intralayer structures. This may be taken as support for the empirical observations above, that it is the intralayer structure that is the robust motif in these structures.

## Experimental

### General procedures

All reactions were performed using standard Schlenk techniques under an atmosphere of dry, oxygen-free dinitrogen. All solvents were distilled from appropriate drying agents immediately prior to use (sodium for $Et_2O$ and hexanes and $CaH_2$ or 3 Å molecular sieves for chlorocarbons). Microanalytical data were obtained at the University of Bristol.

Compounds **6** and **7** were prepared by the literature methods,[3a] **1** and **2** were procured commercially.

### Preparations

In a typical preparation, a pale yellow solution of compound **2** (0.027 g; 0.21 mmol) in $CH_2Cl_2$ (2 $cm^3$) was added to a colourless solution of **6** (0.063 g; 0.21 mmol) in $CH_2Cl_2$ (2 $cm^3$) resulting in no noticeable colour change. This reaction solution was then cooled to −30° C and maintained at this temperature for 24 h. After this time a crop of small dark red crystals had formed. The remaining solution was then removed by syringe and the resulting crystals of **6·2** washed with $Et_2O$ (1 $cm^3$) and hexane (2 × 2 $cm^3$) and dried under vacuum (0.051 g, 56%). One of these was used for X-ray crystallography ($C_9H_4BN_2S_2$ requires C, 50.3; H, 1.9; N, 13.0. Found: C, 50.4; H, 1.8; N, 13.3%). Crystals of **6·2** with the same unit cell dimensions were also obtained from chlorobenzene and 1,2-dichloroethane.

All other compounds were prepared similarly. Crystals of adduct **6·1a** were obtained from $CH_2Cl_2$ solution (60%) ($C_{12}H_6BN_2S_2$ requires C, 56.9; H, 2.4; N, 11.1. Found: C, 58.7; H, 2.5; N, 13.0%), of **6·1b** from 1,2-dichloroethane solution (54%) (Found: C, 57.8; H, 2.7; N, 12.5%), of **7·1** from $CH_2Cl_2$ solution (53%) ($C_{12}H_6BN_2O_2$ requires C, 65.2; H, 2.7; N, 12.7. Found: C, 64.1; H, 2.9; N, 9.6%) and of **7·2** from $CH_2Cl_2$ solution (39%) ($C_9H_4BN_2O_2$ requires C, 59.1; H, 2.2; N, 15.3. Found: C, 57.0; H, 2.4; N, 14.3%). Crystals of **7·2** with the same unit cell as those grown from $CH_2Cl_2$ were also obtained from 1,2-dichloroethane.

### X-Ray crystallography

Many of the details of the structure analyses are listed in Table 1. X-Ray diffraction measurements on single crystals coated in a hydrocarbon oil mounted on a glass fibre under argon were made with graphite-monochromated Mo-Kα X-radiation ($\bar{\lambda}$ = 0.71073 Å) using a Siemens SMART area diffractometer.

CCDC reference number 186/1460.

See http://www.rsc.org/suppdata/dt/1999/2127/ for crystallographic files in .cif format.

### Lattice energy calculations

Atomic point charges for each component molecule were assigned individually using GAUSSIAN[13] at the 6-31G level. Lattice energy calculations were performed on the experimental geometry using the Crystal Packer module in Cerius 2[14] and with unrestricted geometry optimisation with the Dreiding[15] force field.

## Acknowledgements

T. B. M. thanks Natural Sciences and Engineering Research Council of Canada (NSERC), N. C. N. thanks the EPSRC, Laporte plc and The Royal Society and A. G. O. thanks EPSRC for research support and for a studentship (to M. J. Q.). T. B. M. and N. C. N. also thank NSERC and The Royal Society for supporting this collaboration *via* a series of Bilateral Exchange Awards.

## References

1 M. R. Bryce and L. C. Murphy, *Nature* (*London*), 1984, **309**, 119; - J. M. Williams, M. A. Beno, H. H. Wang, P. C. W. Leung, T. J. Emge, U. Geiser and K. D. Carlson, *Acc. Chem. Res.*, 1985, **18**, 261.
2 T. J. Emge, F. Mitchell Wiygul, J. S. Chappell, A. N. Bloch, J. P. Ferraris, D. O. Cowan and T. J. Kistenmacher, *Mol. Cryst. Liq. Cryst.*, 1982, **87**, 137.
3 (*a*) F. J. Lawlor, N. C. Norman, N. L. Pickett, E. G. Robins, P. Nguyen, G. Lesley, T. B. Marder, J. A. Ashmore and J. C. Green, *Inorg. Chem.*, 1998, **37**, 5282; (*b*) W. Clegg, M. R. J. Elsegood, F. J. Lawlor, N. C. Norman, N. L. Pickett, E. G. Robins, A. J. Scott, P. Nguyen, N. J. Taylor and T. B. Marder, *Inorg. Chem.*, 1998, **37**, 5289; (*c*) G. Lesley, T. B. Marder, N. C. Norman and C. R. Rice, *Main Group Chem. News*, 1997, **5**, 4.
4 W. Clegg, C. Dai, F. J. Lawlor, T. B. Marder, P. Nguyen, N. C. Norman, N. L. Pickett, W. P. Power and A. J. Scott, *J. Chem. Soc.*, *Dalton Trans.*, 1997, 839.
5 M. Decoster, F. Lonan, J. E. Guerchais, Y. Le Mist, J. Sala Pala, J. C. Jeffery, E. Faulgues, A. Leblon and P. Molinine, *Polyhedron*, 1995, **14**, 1741.
6 R. E. Long, R. A. Sparks and K. N. Trueblood, *Acta Crystallogr.*, 1965, **18**, 932.
7 R. E. Little, D. Pautler and P. Coppens, *Acta Crystallogr.*, *Sect. B*, 1971, **27**, 1493.
8 U. Druck and H. Guth, *Z. Kristallogr.*, 1982, **161**, 103.
9 J. M. Williams, personal communication; G. R. Whittell, unpublished work.
10 (*a*) R. Docherty and W. Jones, *Organic Molecular Solids, Properties and Applications*, ed. W. Jones, CRC Press, New York, 1997; (*b*) A. Gavezotti and G. Filippini, *J. Am Chem. Soc.*, 1995, **117**, 12299; - (*c*) M. H. Charlton, R. Docherty and M. G. Hutchings, *J. Chem. Soc.*, *Perkin Trans. 2*, 1995, 2203.
11 A. Gavezotti, *J. Am Chem. Soc.*, 1991, **113**, 4622.
12 D. Buttar, M. H. Charlton, R. Docherty and J. Starbuck, *J. Chem. Soc.*, *Perkin Trans. 2*, 1998, 763.
13 GaussView v. 1.01, Gaussian Inc., Semichem, Pittsburgh, 1997.
14 Cerius 2 v. 3.5, Molecular Simulations Inc., Cambridge, 1997.
15 S. L. Mayo, B. D. Olafson and W. A. Goddard (III), *J. Phys. Chem.*, 1990, **94**, 8897.

*Paper 9/01169B*